Free Vibration Analysis of Cracked Euler-Bernoulli Beam by Laplace Transformation Considering Stiffness Reduction

Xingzhuang ZHAO
A. James Clark School of Engineering, University of Maryland, College Park, MD, 20740, United States, E-mail: xzzhao@umd.edu

Abstract: - This work investigates the free vibration of a cracked Euler-Bernoulli beam. The governing equation of motion is formulated by using the stiffness reduction factor and the generalized function to consider the degree of stiffness loss and the location of the crack, respectively. By implementing the centered finite difference method, the singularity problem of the curvature at the cracked cross-section is addressed. The effect of crack location and stiffness reduction factor on the frequencies and the modal shapes is investigated. The proposed method is simple and practical for analyzing the cracked beam.

Keywords: - Euler-Bernoulli beam, vibration, frequency, finite difference method, Laplace transform

1. INTRODUCTION

Crack is an important indicator of damage in civil engineering, mechanical engineering, and aerospace engineering. As a result of the accumulation of cracking in structures, the frequencies and modal shapes will change due to the degradation of the integrity of the structures. Because of this correlation between cracks and frequencies and modal shapes, intensive investigations have been conducted on the direct problem and inverse problem of the vibration-based crack detection technique. The former is defined as analyzing the changes of the dynamic responses of the structures as a result of cracking, and the latter is formulated as detecting the location and depth of the cracks using the measured vibration parameters of the cracked structures. In order to study the reverse problem with high accuracy, the understanding of the effects of the cracks on the vibration responses of structures is critical. As one of the important components in engineering structures, the cracked beam has been actively studied for the past three decades. Many researchers contribute to this topic and some important results are achieved.

The fracture-mechanics-based model was developed to simulate the local stiffness reduction. In this model, the open edge crack was simulated by a massless rotational spring based on the observation that beam stiffness will be reduced in the vicinity of a crack tip. The relationship between the crack depth and the equivalent stiffness massless rotational spring stiffness was constructed to account for the varied strain energy functions obtained via the tests [1, 2]. The massless rotational spring model was implemented by Rizos et al. [3] to link the segments of sub-beams of a cantilever beam separated by the cracks. The equation of motion of each sub-beam was built separately and the four compatibility conditions at the cracking cross-section were considered to find the natural frequencies by solving an eighth-order determinant equation. When the crack number is increased, a significant challenge is imposed for computing efficiency because the order of the determinant would be 4n+4 for a beam with n cracks. To reduce the order of determinant and enhance computing efficiency, Shifrin and Ruotolo [4] reported a new smooth function method to degenerate the order of the determinant to n+2.

The finite element method is an important tool to study the dynamic responses of the cracked beam. Finite element method was adopted by Shen and Pierre [5] to study the natural frequencies of a cracked beam with symmetrical open cracks. Negru et al. [6] studied the distortion effect of the cracking on the neutral axis by the finite element method. The relationship between frequency shift and deflection increase was observed. Implementing the finite element method, Tufisi [7] studied the stiffness degradation effect of branched cracks and investigated the influence of cracking on natural frequency drop. The problem with the finite element method is that the frequencies may change for varied mesh sizes.

The famous Rayleigh-Ritz method was adopted by Fernandez-Saez et al. [8] to investigate the fundamental frequencies of a cracked simply supported beam and a polynomial function was combined with the intact beam to address the varied crack geometries and depths. Zhong and Oyadiji [9] further developed this technique to study the natural frequencies of the arbitrary mode of a cracked simply supported beam impacted by a moving mass.

Most of the above methods were aiming at finding the frequency and did not report the explicit closed-form solution of the modal shape of a cracked beam. Ghannadiasl and Ajirlou [10] studied the dynamic response of the cracked beam by the Green Function

Method, the discontinuity of the beam was simulated by the rotational spring. However, the discontinuity of the slope at the crack cross-section was determined by transmitted bending moment and the massless rotational spring, but the stiffness of which must be determined by tests from fracture mechanics and there are several formulas for rectangular cross-section only.

To obtain the closed-form solution of a vibrating beam with cracks, many mathematical models were proposed. The generalized functions (Heaviside and Dirac's delta function) were utilized and proved to a useful tool to simulate the discontinuities at the crack cross-section of a beam.

Caddemi et al. [11-23] actively investigated the dynamic response of cracked beam by superimposing a sequence of generalized functions to the flexural stiffness to consider the discontinuity at the crack cross-section. The resulted equation of motion can be solved by the virtual of Laplace transform pairs, making the procedure of integration unnecessary. The modal shape can be determined by the boundary conditions. This method is novel and adopted by many researchers, for instance, Yan et al. [24] adopted the generalized functions, the 'damage parameters' and the relationship between the 'damage parameter' and the equivalent rotational stiffness. A closed-form solution was reported in Yan's work by giving four recursive formulas. The problem with this method is that the curvature at the crack cross-section would be infinity. To address this problem, the not-well-defined $\delta^2(x-x_0)$ was required and the relation $\delta^2(x-x_0)=A\delta(x-x_0)$ was used, where A is a constant.

This paper intends to formulate the equation of motion of a cracked beam with the stiffness reduction factor and resolve the singularity of the curvature and the crack cross-section by finite difference method to consider the reduction effect of cracking on stiffness. The proposed method in this paper is efficient and simple to implement. The purpose of this work is to present that the analytical solution can be obtained for the Euler Bernoulli beam with singularity by using finite difference to resolve the curvature singularity problem at the position of the crack.

Compared with the methods used by Yan et al.[24], the 'damage parameters' and equivalent rotational stiffness of the damaged cross-section are unnecessary for this method. Therefore, the relation between the damage parameter and equivalent rotational stiffness will not be used. Besides, the definition of $\delta^2(x-x_0)$ adopted by Yan et al. is unnecessary. The object of this paper is to propose a new simple and practical analytical technique to determine the natural frequency and the modal shape for a locally weakened Euler-Bernoulli beam and address the curvature singularity problem at the cracked cross-section.

2. EQUATION OF MOTION OF CRACKED BEAM

The governing equation of motion for free vibration of a cracked Euler-Bernoulli beam considering the stiffness reduction effect is shown in Eq. (1).

$$\frac{\partial^2}{\partial x^2}\left[E_0 I(x)\frac{\partial^2 y(x,t)}{\partial x^2}\right]+\rho_0 A_0\frac{\partial^2 y(x,t)}{\partial t^2}=0 \quad (1)$$

where: y and x are the deflection and the coordinate along the beam, respectively; E_0 and ρ_0 are Young's modulus and the density of the beam, respectively; $I(x)$ is the moment of inertia, depending on the position; A_0 is the area of the cross-section; t is the time variable.

The abrupt reduction of the stiffness in the beam cross-section due to cracking is simulated by Dirac's delta function. The definition of the Dirac delta function and its first derivative are shown in Eq. (2) and (3) [25].

$$\delta(x-x_0)=\begin{cases}\infty & (x=x_0)\\ 0 & (|x|>x_0)\end{cases} \quad (2)$$

$$\delta'(x-x_0)=\begin{cases}0 & (|x|>x_0)\\ -\infty & (x_0^-)\\ \infty & (x_0^+)\\ 0 & (x=x_0)\end{cases} \quad (3)$$

Replacing the $I(x)$ in Eq. (1) by

$$I(x)=I_0[1-\xi\delta(x-x_0)] \quad (4)$$

where I_0 is the stiffness of the intact beam; $0<x_0<L$ is the position of the crack and L is the total length of the beam; the parameter $0\le\xi<1$, is the stiffness reduction factor. The stiffness reduction increases with ξ; when $\xi=0$, the beam is intact; when ξ is close to 1, the stiffness of the beam at x_0 is lost. It should be pointed out that the stiffness reduction factor ξ in this paper is different from the 'damage parameter' in the work of Yan et al. [24]. The stiffness reduction factor directly reflects the degree of stiffness lost while the damage parameter is related to the equivalent rotational stiffness, which should be determined separately.

Considering the discontinuity imposed to the governing equation (1), the following equation of motion is obtained

$$\frac{\partial^2}{\partial x^2}\left\{E_0 I_0[1-\xi\delta(x-x_0)]\frac{\partial^2 y(x,t)}{\partial x^2}\right\}+\rho_0 A_0\frac{\partial^2 y(x,t)}{\partial t^2}=0 \quad (5)$$

By the method of separation of variables, the form of solution is assumed to be

$$y(x,t) = y(x)e^{i\omega t} \tag{6}$$

Substitution of Eq. (6) into (5), and introduce $\lambda = \sqrt[4]{\omega^2 \frac{\rho_0 A_0}{E_0 I_0}}$, Eq. (6) can be expressed as

$$\frac{\partial^2}{\partial x^2}\left\{[1 - \xi\delta(x - x_0)]\frac{\partial^2 y(x)}{\partial x^2}\right\} - \lambda^4 y(x) = 0 \tag{7}$$

3. ANALYTICAL SOLUTION BY LAPLACE TRANSFORM

The analytical solution of Eq. (7) can be found by the Laplace transform, which is a powerful tool for solving differential equation with Dirac's delta function.

First, define the term in the curly bracket of Eq. (7) by

$$\gamma(x) = [1 - \xi\delta(x - x_0)\,]\frac{\partial^2 y(x)}{\partial x^2} \tag{8}$$

where $\gamma(0) = y''(0)$ and $\gamma'(0) = y'''(0)$ can be achieved by utilizing Eq. (3) and (4).

Performing the Laplace transform of Eq. (8) gives

$$\Gamma(s) = \mathcal{L}\{\gamma(x)\} = s^2Y(s) - sy(0) - y'(0) - \xi e^{-sx_0}y''(x_0) \tag{9}$$

where $Y(s) = \mathcal{L}\{y(x)\}$.

Similarly, the Laplace transform of Eq. (7) results

$$s^2\Gamma(s) - s\gamma(0) - \gamma'(0) - \lambda Y(s) = 0 \tag{10}$$

Combination of Eq. (9) and (10), Eq. (11) is obtained.

$$Y(s) = \frac{s^3y(0)+s^2y'(0)+\xi s^2e^{-sx_0}y''(x_0)+s\gamma(0)+\gamma'(0)}{s^4-\lambda^4} \tag{11}$$

where the four variables $y(0)$, $y'(0)$, $y''(0)$, and $y'''(0)$ can be treated as constants and represent the deflection, slope, moment and shear force, respectively. And $y''(x_0)$ and $y(x_0)$ are the moment and deflection of the beam at x_0, respectively; both can be determined then the modal function $y(x)$ is found.

Performing the inverse Laplace transform, the modal shape function in Eq.(12) is derived

$$y(x) = y(0)\left[\frac{cos(\lambda^{1/4}x)+cosh(\lambda^{1/4}x)}{2}\right] + y'(0)\left[\frac{sin(\lambda^{1/4}x)+sinh(\lambda^{1/4}x)}{2\lambda^{1/4}}\right] - y''(0)\left[\frac{cos\left(\lambda^{\frac{1}{4}}x\right)-\cosh(\lambda^{\frac{1}{4}}x)}{2\lambda^{\frac{1}{2}}}\right] - y'''(0)\left[\frac{sin\left(\lambda^{\frac{1}{4}}x\right)-\sinh(\lambda^{\frac{1}{4}}x)}{2\lambda^{\frac{3}{4}}}\right] + y''(x_0)\xi H(x - x_0)\left\{\frac{sin\left[\lambda^{\frac{1}{4}}(x-x_0)\right]+\sinh\left[\lambda^{\frac{1}{4}}(x-x_0)\right]}{2\lambda^{\frac{1}{4}}}\right\} \tag{12}$$

To simplify the expression in Eq. (12) and facilitate the following calculations the following four functions are defined

$$S_0(\lambda x) = \frac{cos(\lambda x)+cosh(\lambda x)}{2} \tag{13}$$

$$S_1(\lambda x) = \frac{sin(\lambda x)+sinh(\lambda x)}{2\lambda} \tag{14}$$

$$S_2(\lambda x) = \frac{-cos(\lambda x)+\cosh(\lambda x)}{2\lambda^2} \tag{15}$$

$$S_3(\lambda x) = \frac{-sin(\lambda x)+\sinh(\lambda x)}{2\lambda^3} \tag{16}$$

Based on definitions in Eq. (13) - (16) the following relations can be easily checked.

$$\frac{d}{dx}[S_3(\lambda x)] = S_2(\lambda x) \tag{17}$$

$$\frac{d}{dx}[S_2(\lambda x)] = S_1(\lambda x) \tag{18}$$

$$\frac{d}{dx}[S_1(\lambda x)] = S_0(\lambda x) \tag{19}$$

$$\frac{d}{dx}[S_0(\lambda x)] = \lambda^4 S_3(\lambda x) \tag{20}$$

The relationships between the fourth derivative of the equations in Eq. (13) - (16) and the definition are as follows

$$[S_3(\lambda x)]^{iv} = \lambda^4 S_3(\lambda x) \tag{21}$$

$$[S_2(\lambda x)]^{iv} = \lambda^4 S_2(\lambda x) \tag{22}$$

$$[S_1(\lambda x)]^{iv} = \lambda^4 S_1(\lambda x) \tag{23}$$

$$[S_0(\lambda x)]^{iv} = \lambda^4 S_0(\lambda x) \tag{24}$$

Notice that the following results can be easily checked.

$$S_0(0) = 1, S_1(0) = S_2(0) = S_3(0) = \tag{25}$$

By applying the above definitions, Eq. (12) is simplified

$$y(x) = y(0)S_0(\lambda x) + y'(0)S_1(\lambda x) + y''(0)S_2(\lambda x) + y'''(0)S_3(\lambda x) + y''(x_0)\xi H(x - x_0)S_1(\lambda x - \lambda x_0) \tag{26}$$

Taking the second derivation of Eq. (26) and using the property of Dirac's delta function, the curvature at x_0 is written as

$$y''(x_0) = \lambda^4 y'(0) S_3(\lambda x_0) + y'''(0) S_1(\lambda x_0) + 2y''(x_0)\xi \int_0^L \delta^2(x - x_0) S_0(\lambda x - \lambda x_0)\, dx + \lambda^4 y''(x_0)\xi \int_0^L H(x - x_0)\delta(x - x_0) S_3(\lambda x - \lambda x_0) dx + y''(x_0)\xi \int_0^L \delta'(x - x_0)\delta(x - x_0) S_1(\lambda x - \lambda x_0) dx \tag{27}$$

It can be observed from the third term in Eq. (27) that $y''(x_0)$ is infinity. In order to address this problem, Yan et al. [24] adopted the definition $\delta^2(x - x_0) = A\delta(x - x_0)$, which was proposed by Biondi and Caddemi [23, 24]. However, $\delta^2(x - x_0)$ is an open question and is not well defined, although the exact value of the constant A was not used in their papers. In this paper, the curvature at x_0 is approached by the centered finite difference

$$y''(x_0) = \frac{y'(x_0+h) - y'(x_0-h)}{2h} \tag{28}$$

where h is the step-size.

4. ILLUSTRATION OF SIMPLY SUPPORTED BEAM

To show how to find the frequencies and modal functions with the proposed method, a simply supported beam is illustrated in this section.

Assuming the length of the beam is L, and the four boundary conditions are

$$y(0) = y(L) = y''(0) = y''(L) = 0 \tag{29}$$

Substituting $y(0) = y''(0) = 0$ into Eq. (11), we arrive at

$$y(x) = y'(0) S_1(\lambda x) + y'''(0) S_3(\lambda x) + y''(x_0)\xi H(x - x_0) S_1(\lambda x - \lambda x_0) \tag{30}$$

Considering the boundary conditions in Eq. (31) and the property of the Dirac delta function in Eq. (32), Eq. (33) - (36) are obtained.

$$\begin{cases} y(x)|_{x=L} = 0 \\ y''(x)|_{x=L} = 0 \end{cases} \tag{31}$$

$$\begin{cases} \int_0^L y(x)\delta(x - L)dx = 0 \\ \int_0^L y''(x)\delta(x - L)dx = 0 \\ \int_0^L y(x)\delta(x - x_0)dx = y(x_0) \\ \int_0^L y''(x)\delta(x - x_0)dx = y''(x_0) \end{cases} \tag{32}$$

$$y(L) = y'(0) S_1(\lambda L) + y'''(0) S_3(\lambda L) + y''(x_0)\xi S_1(\lambda L - \lambda x_0) = 0 \tag{33}$$

$$y''(L) = y'(0)\lambda^4 S_3(\lambda L) + y'''(0) S_1(\lambda L) + y''(x_0)\xi\lambda^4 S_3(\lambda L - \lambda x_0) = 0 \tag{34}$$

$$y'(x_0 + h) = y'(0) S_0(\lambda x_0 + \lambda h) + y'''(0) S_2(\lambda x_0 + \lambda h) + y''(x_0)\xi S_0(\lambda h) \tag{35}$$

$$y'(x_0 - h) = y'(0) S_0(\lambda x_0 - \lambda h) + y'''(0) S_2(\lambda x_0 - \lambda h) \tag{36}$$

Solving for $y(x_0)$ and $y''(x_0)$, Eq. (37) is obtained and solving for $y(L)$ and $y''(L)$, Eq. (39) is arrived at.

$$\begin{pmatrix} y(x_0) \\ y''(x_0) \end{pmatrix} = C \begin{pmatrix} y'(0) \\ y'''(0) \end{pmatrix} \tag{37}$$

where C is defined as

$$C = \begin{bmatrix} C_{11} & C_{12} \\ C_{21} & C_{22} \end{bmatrix} \tag{38}$$

in which $C_{11} = S_1(\lambda x_0)$, $C_{12} = S_3(\lambda x_0)$,
$C_{21} = [S_0(\lambda x_0 + \lambda h) - S_0(\lambda x_0 - \lambda h)]/[2h - \xi S_0(\lambda h)]$,
$C_{22} = [S_2(\lambda x_0 + \lambda h) - S_2(\lambda x_0 - \lambda h)]/[2h - \xi S_0(\lambda h)$

$$\begin{pmatrix} y(L) \\ y''(L) \end{pmatrix} = A \begin{pmatrix} y'(0) \\ y'''(0) \end{pmatrix} + B \begin{pmatrix} y(x_0) \\ y''(x_0) \end{pmatrix} \tag{39}$$

where

$$A = \begin{bmatrix} S_1(\lambda L) & S_3(\lambda L) \\ \lambda^4 S_3(\lambda L) & S_1(\lambda L) \end{bmatrix} \tag{40}$$

$$B = \begin{bmatrix} 0 & \xi S_1(\lambda L - \lambda x_0) \\ 0 & \xi\lambda^4 S_3(\lambda L - \lambda x_0) \end{bmatrix} \tag{41}$$

Substituting Eq. (37) into (39) and setting the determinant equal to zero, Eq. (42) is obtained.

$$\det(A + BC) = 0 \tag{42}$$

It is worth noting that after λ is solved from Eq. (42), the frequencies of the cracked beam can be determined correspondingly.

In order to find the modal shape function, Eq. (43) is selected from Eq. (39)

$$y(L) = y'(0) A_{11} + y'''(0) A_{12} = 0 \tag{43}$$

where

$$A_{11} = S_1(\lambda L)[2h - \xi S_0(\lambda h)] + \xi S_1(\lambda L - \lambda x_0)[S_0(\lambda x_0 + \lambda h) - S_0(\lambda x_0 - \lambda h)] \tag{44}$$

$$A_{12} = S_3(\lambda L)[2h - \xi S_0(\lambda h)] + \xi S_1(\lambda L - \lambda x_0)[S_2(\lambda x_0 + \lambda h) - S_2(\lambda x_0 - \lambda h)] \tag{45}$$

Assuming $\sqrt{y'(0)^2 + y'''(0)^2} = 1$, then $y'''(0)$ and $y'(0)$ are obtained.

$$\boldsymbol{y'''(0)} = \frac{A_{11}}{\sqrt{A_{12}^2 + A_{11}^2}} \quad (46)$$

$$y'(0) = -\frac{A_{12}}{\sqrt{A_{12}^2 + A_{11}^2}} \quad (47)$$

In view of Eq. (44) - (47), the modal shape function is

$$\boldsymbol{y(x) = y'(0)\{S_1(\lambda x) + \xi H(x - x_0)S_1(\lambda x - \lambda x_0)[S_0(\lambda x_0 + \lambda h) - S_0(\lambda x_0 - \lambda h)]/[2h - \xi S_0(\lambda h)]\} + y'''(0)\{S_3(\lambda x) + \xi H(x - x_0)S_1(\lambda x - \lambda x_0)[S_2(\lambda x_0 + \lambda h) - S_2(\lambda x_0 - \lambda h)]/[2h - \xi S_0(\lambda h)]\}} \quad (48)$$

5. NUMERICAL EXAMPLE

To illustrate and verify the proposed method, a cracked concrete beam is investigated in this section. The properties of the simply supported beam are as follows: length $L = 20$ m, Young's modulus $E_0 = 20$ GPa, width $b = 0.8$ m, and height $h_0 = 1$ m.

Three crack locations are considered: $0.1L$, $0.3L$ and $0.5L$. The stiffness reduction factors for each crack location are: 0.15, 0.3, 0.45, and 0.6.

Table 1 First natural frequency (Hz)

		This paper	Rayleigh-Ritz	Error (%)	This paper	Rayleigh-Ritz	Error (%)	This paper	Rayleigh-Ritz	Error (%)
Crack position		$0.1L$			$0.3L$			$0.5L$		
Stiffness reduction factor	0	3.27	3.27	0.00	3.27	3.27	0.00	3.27	3.27	0.00
	0.15	3.27	3.27	0.03	3.25	3.26	0.22	3.24	3.25	0.33
	0.30	3.27	3.27	0.05	3.23	3.24	0.37	3.20	3.22	0.58
	0.45	3.26	3.26	0.06	3.20	3.22	0.46	3.17	3.19	0.72
	0.60	3.26	3.26	0.05	3.18	3.19	0.46	3.13	3.16	0.76

Table 2 Second natural frequency (Hz)

		This paper	Rayleigh-Ritz	Error (%)	This paper	Rayleigh-Ritz	Error (%)	This paper	Rayleigh-Ritz	Error (%)
Crack position		$0.1L$			$0.3L$			$0.5L$		
Stiffness reduction factor	0	13.09	13.09	0.00	13.09	13.09	0.00	13.09	13.09	0.00
	0.15	13.04	13.05	0.11	12.96	13.00	0.29	13.09	13.09	0.00
	0.30	12.99	13.01	0.19	12.84	12.90	0.48	13.09	13.09	0.00
	0.45	12.94	12.97	0.21	12.73	12.80	0.56	13.09	13.09	0.00
	0.60	12.89	12.91	0.18	12.62	12.69	0.52	13.09	13.09	0.00

Table 3 Third natural frequency (Hz)

		This paper	Rayleigh-Ritz	Error (%)	This paper	Rayleigh-Ritz	Error (%)	This paper	Rayleigh-Ritz	Error (%)
Crack position		$0.1L$			$0.3L$			$0.5L$		
Stiffness reduction factor	0	29.45	29.45	0.00	29.45	29.45	0.00	29.45	29.45	0.00
	0.15	29.24	29.30	0.21	29.42	29.43	0.03	29.13	29.23	0.32
	0.30	29.03	29.13	0.34	29.39	29.41	0.05	28.84	28.99	0.53
	0.45	28.83	28.94	0.37	29.37	29.38	0.05	28.57	28.75	0.62
	0.60	28.64	28.72	0.28	29.34	29.36	0.05	28.33	28.49	0.57

The eigenvalues corresponding to the natural frequencies can be solved from Eq. (42). The numerical values for the first three natural frequencies are shown in

Table 1 - Table 3. The Rayleigh-Ritz method [8] is used to calculate the frequencies for comparison, and the calculated results are tabulated in the table. The results suggest that the proposed method in this paper works well, as the calculated frequencies are close to that by the Rayleigh-Ritz method.

It is observed that the natural frequency is decreasing when the stiffness reduction factor is increasing except for the third natural frequency when the crack is at the middle point of the beam. This is because the cracked cross-section is the inflection point of the third mode [24]. For the same stiffness factor, the first and second natural frequency is decreasing when the crack is moving from the end to the middle of the beam, which indicates cracking in near the center of the beam tends to produce a more significant influence on the first and second natural frequency of the beam.

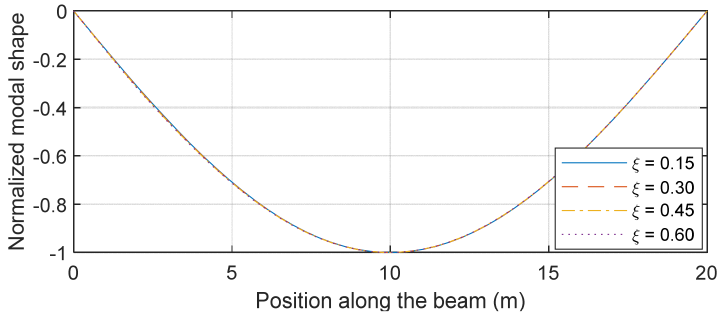

(a)

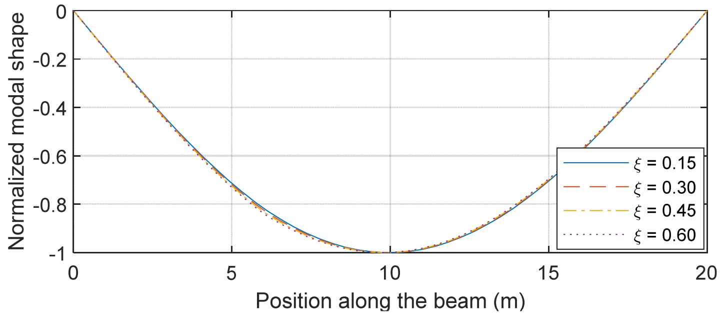

(b)

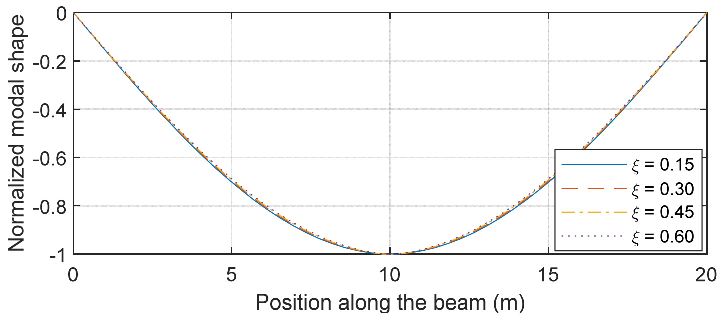

(c)

Figure 1. The modal shape of the first frequency. (a) $\boldsymbol{x_0 = 0.1L}$, (b) $\boldsymbol{x_0 = 0.3L}$, (c) $\boldsymbol{x_0 = 0.5L}$.

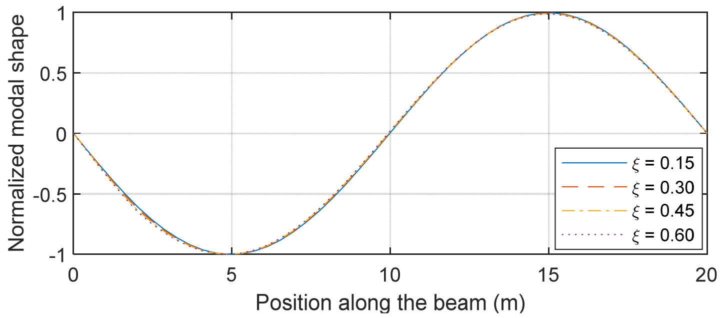

(a)

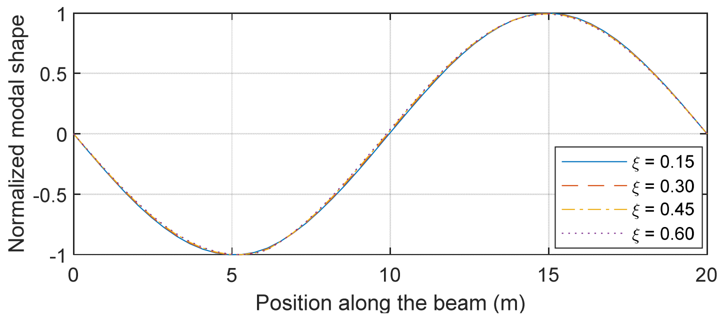

(b)

Figure 2. (a, b) The modal shape of the second frequency. (a) $x_0 = 0.1L$, (b) $x_0 = 0.3L$

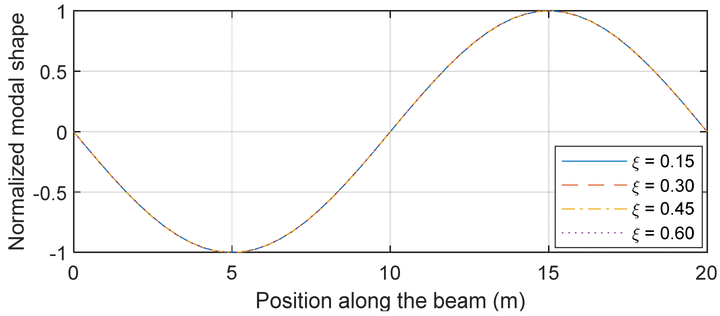

(c)

Figure 2. (c) The modal shape of the second frequency. (c) $x_0 = 0.5L$.

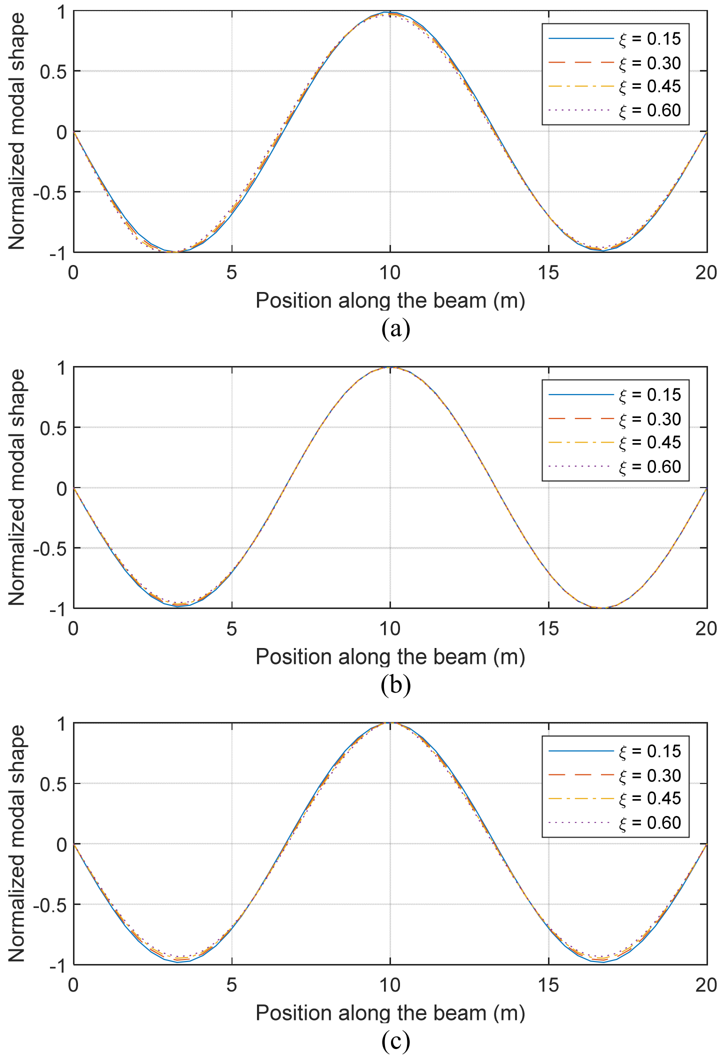

Figure 3. The modal shape of the third frequency. (a) $x_0 = 0.1L$, (b) $x_0 = 0.3L$, (c) $x_0 = 0.5L$.

The modal shapes are achieved by implementing Eq. (48), and the modal shapes for the three crack locations corresponding to varied stiffness reduction factors are shown in Figure 1- Figure 3.

6. CONCLUSIONS

In this paper, the crack in a Euler-Bernoulli beam is simulated by a generalized function and Laplace transform pairs are implemented to derive the modal shape function. In formulating the governing equation of motion, the stiffness reduction factor is introduced to consider the level of stiffness loss. The proposed method is verified by utilizing the Rayleigh-Ritz method. The main results achieved by this investigation are summarized as follows: (a) the singularity of the curvature of the beam at the cracked cross-section is addressed by utilizing the centered-finite difference method; (b) the stiffness reduction factor is directly utilized to represent the stiffness loss in the governing equation of motion; (c) the frequencies and modal shapes corresponding to varied stiffness reduction factors and different crack locations can be obtained by the proposed method. The method in this work is simple and practical and potentially useful for identifying cracking in a beam.

REFERENCES

[1] Ostachowicz W, Krawczuk M., *Analysis of the effect of cracks on the natural frequencies of a cantilever beam*, Journal of Sound and Vibration, Vol.150, No.2, 1991, pp. 191-201.

[2] Labib A, Kennedy D, Featherston C., *Free vibration analysis of beams and frames with multiple cracks for damage detection*, Journal of Sound and Vibration, Vol.333, No.20, 2014, pp. 4991-5003.

[3] Rizos P, Aspragathos N, Dimarogonas A., *Identification of crack location and magnitude in a cantilever beam from the vibration modes*, Journal of Sound and Vibration, Vol.138, No.3, 1990, pp. 381-388.

[4] Shifrin E, Ruotolo R., *Natural frequencies of a beam with an arbitrary number of cracks*, Journal of Sound and Vibration, Vol.222, No.3, 1999, pp. 409-423.

[5] Shen M-H, Pierre C. *Natural modes of Bernoulli-Euler beams with symmetric cracks*, Journal of Sound and Vibration, Vol.138, No.1, 1990, pp. 115-134.

[6] Negru I, Praisach Z-I, Gillich G-R, Vasile O., *About the Neutral Axis Distortion due to Cracks and its Influence upon the Beams Natural Frequencies*, Romanian Journal of Acoustic and Vibration, Vol. 12, Issue 1, 2015, pp. 35-38.

[7] Tufisi C., Gillich G-R, Hamat C.O., Gillich N., Praisach Z-I., *Numerical Study of the Stiffness Degradation Caused by Branched Cracks and its Influence on the Natural Frequency Drop,* Romanian Journal of Acoustic and Vibration, Vol. 15, Issue 1, 2018, pp. 53-57.

[8] Fernandez-Saez J, Rubio L, Navarro C., *Approximate calculation of the fundamental frequency for bending vibrations of cracked beams*, Journal of Sound and Vibration, Vol.225, No.2, 1999, pp. 345-352.

[9] Zhong S, Oyadiji SO., *Analytical predictions of natural frequencies of cracked simply supported beams with a stationary roving mass*, Journal of Sound and Vibration, Vol.311, No.1-2, 2008, pp. 328-352.

[10] Ghannadiasl A, Ajirlou SK., *Analytical Solution of Dynamic Analysis of Cracked Euler-Bernoulli Beam with Elastic Boundary Condition By G.F.M*, Romanian Journal of Acoustic and Vibration, Vol. 15, Issue 2, 2018, pp. 100-107.

[11] Caddemi S, Morassi A., *Multi-cracked Euler–Bernoulli beams: Mathematical modeling and exact solutions*, International Journal of Solids and Structures, Vol.50, No.6, 2013, pp. 944-956.

[12] Caddemi S, Caliò I, Cannizzaro F, Rapicavoli D., *A novel beam finite element with singularities for the dynamic analysis of discontinuous frames*, Archive of Applied Mechanics, Vol.83, No.10, 2013, pp. 1451-1468.

[13] Caddemi S, Caliò I, Cannizzaro F., *Influence of an elastic end support on the dynamic stability of Beck′ s column with multiple weak sections*, International Journal of Non-Linear Mechanics, Vol.69, 2015, pp. 14-28.

[14] Caddemi S, Caliò I, Cannizzaro F., *Tensile and compressive buckling of columns with shear deformation singularities*, Meccanica, Vol.50, No.3, 2015, pp. 707-720.

[15] Caddemi S, Caliò I, Cannizzaro F., *The influence of multiple cracks on tensile and compressive buckling of shear deformable beams*, International Journal of Solids and Structures, Vol.50, No.20-21, 2013, pp. 3166-3183.

[16] Caddemi S, Caliò I, Cannizzaro F., *Closed-form solutions for stepped Timoshenko beams with internal singularities and along-axis external supports*, Archive of Applied Mechanics, Vol.83, No.4, 2013, pp. 559-577.

[17] Caddemi S, Caliò I., *The exact stability stiffness matrix for the analysis of multi-cracked frame structures*, Computers & Structures, Vol.125, 2013, pp. 137-144.

[18] Caddemi S, Caliò I., *The exact explicit dynamic stiffness matrix of multi-cracked Euler–Bernoulli beam and applications to damaged frame structures*, Journal of Sound and Vibration, Vol.332, No.12, 2013, pp. 3049-3063.

[19] Caddemi S, Caliò I., *The influence of the axial force on the vibration of the Euler–Bernoulli beam with an arbitrary number of cracks*, Archive of Applied Mechanics, Vol.82, No.6, 2012, pp. 827-839.

[20] Caddemi S, Calio I., *Exact closed-form solution for the vibration modes of the Euler–Bernoulli beam with multiple open cracks*, Journal of Sound and Vibration, Vol.327, No.3-5, 2009, pp. 473-489.

[21] Caddemi S, Calio I., *Exact solution of the multi-cracked Euler–Bernoulli column*, International Journal of Solids and Structures, Vol.45, No.5, 2008, pp. 1332-1351.

[22] Biondi B, Caddemi S., *Euler–Bernoulli beams with multiple singularities in the flexural stiffness*, European Journal of Mechanics-A/Solids, Vol.26, No.5, 2007, pp. 789-809.

[23] Biondi B, Caddemi S., *Closed form solutions of Euler–Bernoulli beams with singularities*, International Journal of Solids and Structures, Vol.42, No.9-10, 2005, pp. 3027-3044.

[24] Yan Y, Ren Q, Xia N, Zhang L., *A closed-form solution applied to the free vibration of the Euler-Bernoulli beam with edge cracks*: Springer; 2016.

[25] Bracewell RN, Bracewell RN., *The Fourier transform and its applications*: McGraw-Hill New York; 1986.